

Crystal Energy Landscape of Nifedipine by Experiment and Computer Prediction

Published as part of a *Crystal Growth and Design* virtual special issue in Celebration of the Career of Roger Davey

Yue Gui,* Yingdi Jin, Shigang Ruan, Guangxu Sun, Vilmalí López-Mejías, and Lian Yu*



Cite This: *Cryst. Growth Des.* 2022, 22, 1365–1370



Read Online

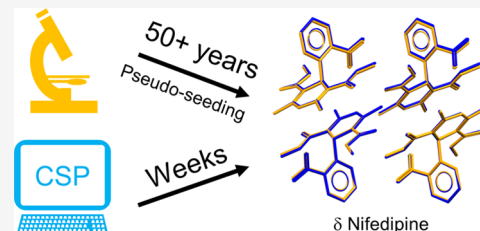
ACCESS |

Metrics & More

Article Recommendations

Supporting Information

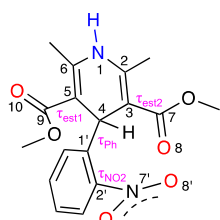
ABSTRACT: The six polymorphs of nifedipine (NIF) known at present have been discovered over the past 50 years, and the most recent one (δ), discovered in 2020, came from an unusual route. This polymorph is ranked second in thermodynamic stability but evaded all previous workers until its melt was seeded with the crystal of a foreign substance, felodipine, in which the molecule has a different conformation from all other NIF polymorphs known at that time. Given this unusual discovery in the lab, we investigated whether crystal structure prediction (CSP) can find this and other polymorphs in a “routine” search. We show that our CSP finds all ordered polymorphs of NIF known at present as low-energy structures (Ranks 1, 3, 4, and 43), including the most recent one unveiled by pseudoseeding (Rank 4). NIF being a flexible molecule, it is of interest to learn which of its many conformers provides the best building block for crystals. An experimental investigation of this question is limited by *survival*; that is, information exists on the structures that are observed but not on those that are difficult to observe or not yet discovered. In this regard, our “computer experiments” access the full range of possibilities. We find that the *syn*periplanar (*sp*) conformer with respect to phenyl torsion produces lower-energy crystals than the *anti*periplanar (*ap*) conformer, with the most stable *ap* crystal being 4 kJ/mol higher in energy than the most stable *sp* structure. Experimentally, the *sp* conformer dominates the *ap* in solution and is the only conformer observed in crystals. With respect to the ester torsions, the *cis/trans* conformer produces the lowest-energy crystals, followed by the *cis/cis* conformer and by the *trans/trans* conformer. Experimentally, five of the six known polymorphs contain the *cis/trans* conformer, one contains the *cis/cis* conformer, and none contain the *trans/trans* conformer. Overall, the CSP is remarkably successful in predicting the polymorphs of NIF in spite of its complex conformational space and provides a quantitative assessment of the relative costs of employing different conformers as units of crystal building.



INTRODUCTION

Nifedipine (NIF, Chart 1) is one of the World Health Organization's Essential Medicines¹ and a prototypical 1,4-

Chart 1. Structure of Nifedipine (NIF)^a



^aThe major torsion angles: τ_{Ph} (C5–C4–C1’–C2’), τ_{NO_2} (C1’–C2’–N7’–O8’), $\tau_{\text{est}1}$ (C6–C5–C9–O10), and $\tau_{\text{est}2}$ (C2–C3–C7–O8). An ester group is *cis* if $\tau_{\text{est}} \approx 0^\circ$ and *trans* if $\tau_{\text{est}} \approx \pm 180^\circ$. The phenyl orientation is *syn*periplanar (*sp*) if the nitro group points in the same direction as C4–H and *anti*periplanar (*ap*) if it points in the opposite direction.

dihydropyridine calcium channel blocker for treating hypertension and angina.² The molecule has significant conformational flexibility with major torsional angles being $\tau_{\text{est}1}$, $\tau_{\text{est}2}$, τ_{Ph} , and τ_{NO_2} (Chart 1). Recognized as polymorphic in the 1970s,³ the number of NIF polymorphs has grown over time (Table 1), now standing at six.^{4–6} Among these, the most recent discovery, δ NIF,⁶ is especially intriguing. Despite being the second most stable of the six forms, δ NIF was not observed under a wide range of crystallization conditions until Gui et al. introduced “pseudo-seeds” into molten NIF.⁶ In their experiment, a melt of NIF was seeded with the crystal of a foreign substance (felodipine) in which the molecule has a different conformation from all polymorphs of NIF known at

Received: November 9, 2021

Revised: December 21, 2021

Published: January 10, 2022



Table 1. Crystal Structures of NIF Polymorphs Known at Present^a

form	α		β		β'	γ	γ'		δ	
T, K	100	297	100	296	338	100	250	296	100	293
CSD ref code	BICCIZ14	BICCIZ07	BICCIZ02	BICCIZ03	BICCIZ08	BICCIZ09	BICCIZ11	BICCIZ10	BICCIZ12	BICCIZ13
$a, \text{\AA}$	10.567	10.929	9.666	9.840	9.696	19.065	11.435	11.450	11.905	12.025
$b, \text{\AA}$	10.408	10.304	13.701	13.807	14.231	11.506	12.244	12.301	10.908	11.238
$c, \text{\AA}$	14.788	14.812	14.118	14.206	14.463	15.109	12.327	12.356	12.779	12.827
α, deg	90	90	61.03	61.39	61.90	90	75.54	75.63	90	90
β, deg	95.03	93.17	79.63	79.76	80.40	108.96	89.06	89.09	106.98	107.65
γ, deg	90	90	81.90	81.99	81.80	90	84.77	84.93	90	90
$V, \text{\AA}^3$	1620.15	1665.47	1605.89	1664.10	1731.05	3134.48	1664.21	1679.19	1587.14	1651.84
sp grp	$P2_1/c$	$P2_1/c$	$\bar{P}1$	$\bar{P}1$	$\bar{P}1$	$P2_1/c$	$\bar{P}1$	$\bar{P}1$	$P2_1/n$	$P2_1/n$
$\rho, \text{g/cm}^3$	1.420	1.381	1.432	1.382	1.329	1.468	1.382	1.370	1.449	1.393
Z/Z'	4/1	4/1	4/2	4/2	4/2	8/2	4/2	4/2	4/1	4/1
R %	3.55	4.73	4.39	5.47	6.69	5.76	4.63	4.38	3.82	4.35

^aMolecular formula: $\text{C}_{17}\text{H}_{18}\text{N}_2\text{O}_6$. Molecular weight: 346.33 g/mol. See the CSD for the complete list of NIF structures under ref. code BICCIZ.

the time. This led to the nucleation and growth of δ NIF in which NIF adopts the same conformation as the seed crystal.

The story of NIF polymorphs is not unique. There have been other reports of the unexpected appearance (and disappearance) of polymorphs,^{7,8} with the new polymorphs being less or more stable than the previous ones.^{9,10} The NIF story fascinates in regard to the role of molecular conformation. Before Gui et al., the previous crystallization conditions only accessed part of the conformational space, while pseudoseeding gained access to another part. This type of experimental search is guided by chemical intuition and is not easily generalized. In contrast, the crystal structure prediction (CSP) approach^{11–13} can in principle search the full conformational space in the discovery of polymorphs. In this work, a CSP was performed to determine whether the δ polymorph of NIF, discovered by an exotic route in the lab, can be discovered in a “routine” search by computers. The results would help assess the likelihood of polymorphs evading laboratory discovery.

We report that the CSP successfully finds all ordered polymorphs of NIF, while the two disordered polymorphs fall outside the current search space. The most stable experimental form (α) is the lowest-energy predicted structure. It is significant that the elusive δ polymorph is identified as a low-energy structure (Rank 4). This straightforward unveiling of a “hidden” polymorph capitalizes on the ability of the CSP to explore the full conformational space. These “computer experiments” also enabled investigations of the energetic costs of employing different conformers as building blocks of crystals.

■ COMPUTATIONAL METHODS

The CSP calculations were conducted using an integrated cloud platform.¹⁴ Gas-phase molecular conformations and energies were calculated at the level B3LYP/6-31G(d), and the results were used to fit the system-specific force-field parameters. Crystal structures were searched with $Z' = 1$ and 2 using a global optimization method that combines the particle swarm optimization (PSO) method and the Monte Carlo (MC) algorithm. On the basis of the Cambridge Structural Database (CSD) statistics, the $Z' = 1$ search included 12 space groups ($\bar{P}1$, $P2/c$, $P2_1/c$, $C2/c$, $P2_12_12$, $P2_12_12$, $Pca2_1$, $Pna2_1$, $Aea2$, $Pccn$, $Pbcn$, $Pbca$), and the $Z' = 2$ search included 9 space groups ($\bar{P}1$, $P2_1$, Cc , $P2_1/c$, $C2/c$, $P2_12_12$, $Pca2_1$, $Pna2_1$, $Pbca$). During the search, the lattice parameters, molecular positions and orientations, and major torsional angles were allowed to vary. Lattice energies were

calculated initially using a system-specific force field to return hits within 40 kJ/mol of the global minimum. Lattice energies were then optimized at the DFT level using VASP^{15–17} during which unit-cell parameters, torsional angles, and molecular positions and orientations were all allowed to vary. The geometries and energies were optimized using the Perdew–Burke–Ernzerhof functional¹⁸ with dispersion correction.¹⁹ Crystal structures were ranked by lattice energies, and the structures within 10 kJ/mol of the global minimum were reported.

To compare the similarities between the predicted and the observed crystal structures, a cluster of 15 molecules from each were overlaid using the software Mercury. The two structures are deemed a match if the root mean-square deviation for the cluster (RMSD₁₅) is smaller than 1 Å. An RMSD₁₅ value smaller than 0.3 Å is considered an excellent match.

■ RESULTS

NIF has six known polymorphs at present (Table 1).⁶ Form α is the most stable at all temperatures and obtained using both solution crystallization and melt crystallization. The metastable forms β and γ and their high-temperature, disordered counterparts β' and γ' were discovered by melt crystallization.²⁰ It is noteworthy that δ NIF is thermodynamically the second most stable form below ca. 360 K but was unknown until 2020 when Gui et al. seeded the melt of NIF with the crystal of felodipine, an analogue of NIF.⁶ Of the six polymorphs, δ NIF is the only one in which the molecule has *cis/cis* conformation with respect to the torsions of the two ester groups (see Chart 1), which happens to be the conformation of the felodipine seed crystal, while all other polymorphs contain the *cis/trans* conformer.

The CSP resulted in 155 predicted crystal structures with lattice energies within 10 kJ/mol of the global minimum, including 59 with $Z' = 1$ and 96 with $Z' = 2$. The results are displayed in Figure 1; the list of structures and the corresponding CIF files are in the Supporting Information.

Table 2 compares the experimental structures of NIF polymorphs with the corresponding CSP hits. The CSP found all NIF polymorphs without disorder, namely, α , β , γ , and δ , as Rank 1, 3, 43, and 4, respectively; these structures are indicated by the red open symbols in Figure 1. There is reasonable agreement between the predicted and the observed unit-cell constants. In Table 2, RMSD₁₅ is the root-mean-square deviation for the overlay of 15 molecules in the predicted and the observed structures. These overlays are shown in Figure 2.

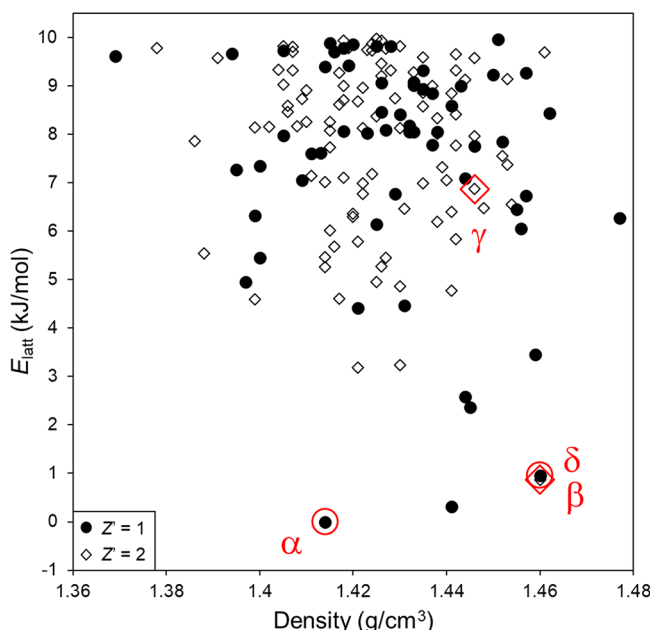


Figure 1. Relative lattice energy plotted against density for predicted crystal structures of NIF with $Z' = 1$ (solid circle) and 2 (open diamond) within 10 kJ/mol relative to the global minimum. The red circles and diamonds indicate the structures that correspond to the experimental polymorphs (see Table 1).

The lowest-energy predicted structure (Rank 1) matches α NIF, the most stable polymorph, with $\text{RMSD}_{15} = 0.203 \text{ \AA}$, indicating an excellent match. That α NIF is the lowest-energy structure is in agreement with its largest enthalpy of melting of all the polymorphs (after accounting for the solid-state transformations in the β and γ polymorphs).⁶ The CSP identified δ NIF as Rank 4 (Rank 3 within $Z' = 1$), with $\text{RMSD}_{15} = 0.159 \text{ \AA}$. In the $Z' = 2$ search space, the CSP identified β and γ as the lowest and 26th lowest-energy structures (Rank 3 and 43 overall). The corresponding RMSD_{15} values are larger (0.490 and 0.368 \AA) but still represent acceptable matches. The two high-temperature, disordered polymorphs, β' and γ' , fall outside the CSP search space. It is worth noting that the CSP of this work was a “blind test” with respect to δ NIF. While the structures of the other polymorphs had been published, the CSP team was unaware of the δ NIF structure. Consistent with experiments, the CSP

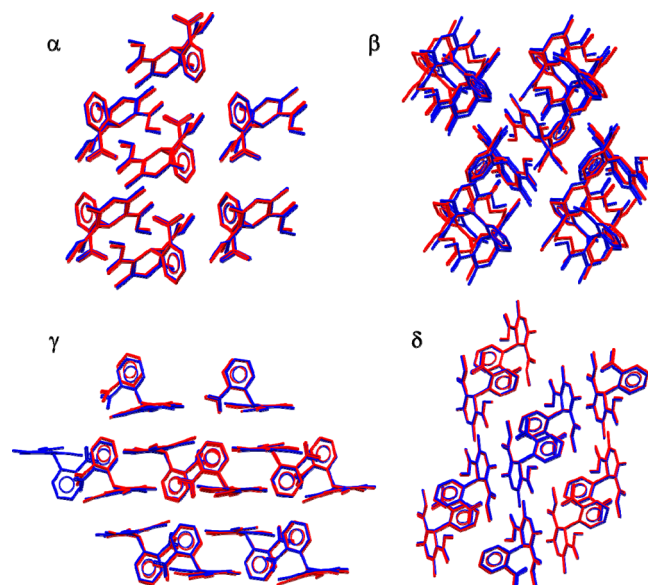


Figure 2. Overlay of predicted (red) and experimental structures (blue) for a cluster of 15 molecules in α , β , γ , and δ NIF viewed along the b axis.

finds δ NIF to have the *cis/cis* conformation, unlike all other known NIF polymorphs (*cis/trans*). Considering the long time and the unusual route (pseudoseeding) to discover this polymorph, its straightforward unveiling by CSP highlights the potential for the CSP to cover experimental blind spots. The successful prediction of δ NIF in a new region of the conformational space, as well as the recovery of all known polymorphs, demonstrates the excellent performance of the CSP method.

Energetic Costs of Using Different Conformers as Units of Crystal Building. Figure 3 shows the energy landscape for the $Z' = 1$ search results where the points are color-coded to indicate the constituent conformer with respect to the two ester torsions (Chart 1). Among the 59 structures, 35 (59%) contain the *cis/trans* conformer, 19 (32%) contain the *cis/cis* conformer, and 5 (8%) contain the *trans/trans* conformer. That is, the *cis/trans* conformer is used most frequently to build crystals, followed by *cis/cis* and by *trans/trans*. One way to evaluate the relative energies of the crystals produced by these conformers is to compare the five lowest-energy structures of each conformer. By this measure, the

Table 2. Comparison of Experimental and Predicted Structures of NIF^a

form	α		β		γ		δ	
	CSD ref code	CSP rank	CSD ref code	CSP rank	CSD ref code	CSP rank	CSD ref code	CSP rank
T, K	BICCIZ14	Rank 01	BICCIZ02	Rank 03	BICCIZ09	Rank 43	BICCIZ12	Rank 04
$a, \text{\AA}$	100	0	100	0	100	0	100	0
$b, \text{\AA}$	10.567	10.439	9.666	9.092	19.065	19.038	11.905	11.904
$c, \text{\AA}$	10.408	10.568	13.701	14.026	11.506	11.521	10.908	10.758
α, deg	14.788	14.826	14.118	14.127	15.109	15.184	12.779	12.948
β, deg	90	90	61.03	62.82	90	90	90	90
γ, deg	95.03	95.84	79.63	81.71	108.96	107.23	106.98	108.14
sp group	$P2_1/c$	$P2_1/c$	$\bar{P}1$	$\bar{P}1$	$P2_1/c$	$P2_1/c$	$P2_1/n$	$P2_1/n$
Z/Z'	4/1	4/1	4/2	4/2	8/2	8/2	4/1	4/1
$\rho, \text{g/cm}^3$	1.420	1.414	1.432	1.460	1.468	1.446	1.449	1.460
$\text{RMSD}_{15}, \text{\AA}$		0.203		0.490		0.368		0.159

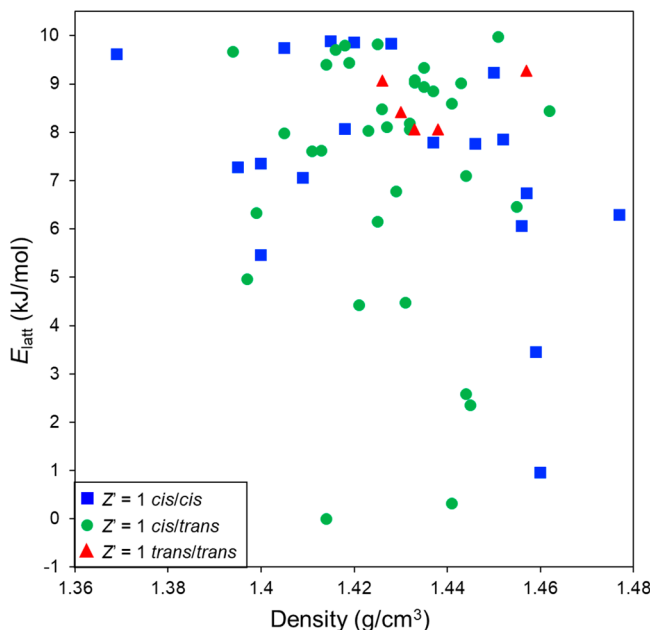


Figure 3. Crystal energy landscape color-coded to show the distribution of conformers arising from the ester torsions. The $Z' = 1$ search space results are shown in which the possible conformers are *cis/cis*, *cis/trans*, and *trans/trans* represented by blue squares, green circles, and red triangles, respectively.

crystals of the *cis/cis* and the *trans/trans* conformers are +4 kJ/mol and +8 kJ/mol higher in energy, respectively, than those of the *cis/trans*. The conformer distribution is more complex in the $Z' = 2$ case given that the two symmetry-independent molecules can have different conformations. But ignoring this difference, we find that the *cis/trans* conformer is employed the most often in the $Z' = 2$ structures (80%) followed by *cis/cis* (18%) and by *trans/trans* (2%), similar to the $Z' = 1$ case.

The distribution of conformers in the predicted structures is consistent with the experimental finding that, of the six known polymorphs of NIF, five contain the *cis/trans* conformer, one contains the *cis/cis* conformer, and none contain the *trans/trans* conformer. It is also in agreement with a survey of 26 crystal structures of dihydropyridine-type NIF analogues, which contain the *cis/trans* or the *cis/cis* conformer and never the *trans/trans*.²¹ In this context, our CSP results are data from “computer experiments” and help assess the energetic cost of using a given conformer as unit of crystal building. Such experiments would be difficult to perform in the laboratory; for example, the *trans/trans* conformer has not been observed in any NIF polymorphs known to date but can be “observed” in computers.

It is noteworthy that the preference for the *cis/trans* conformer in the crystalline state appears to be different from that in the gas phase. According to DFT calculations,⁶ the *cis/cis* conformer has the lowest energy in the gas phase, followed by *cis/trans* (+12 kJ/mol) and by *trans/trans* (+24 kJ/mol). This means that despite its high conformational energy, the *cis/trans* conformer is more commonly used as a building block of crystals, leading to lower-energy structures (Figure 3).

Figure 4 shows the crystal energy landscape for $Z' = 1$ with data points color-coded to indicate the *sp* and *ap* conformers associated with phenyl torsion (Chart 1). Of the 59 structures, 48 (81%) contain the *sp* conformer, and 11 (19%) contain the

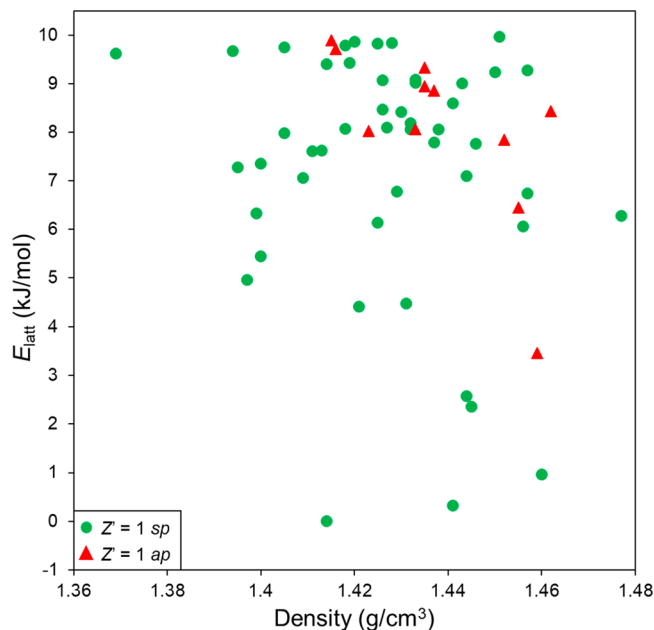


Figure 4. Crystal energy landscape color-coded to show the distribution of conformers arising from phenyl torsion (*sp* and *ap* for the $Z' = 1$ search space results).

ap conformer. Thus, the *sp* conformer is used far more frequently as a unit of crystal building. The *sp* crystals have lower energies than the *ap* crystals. For example, the lowest-energy *ap* crystal is +4 kJ/mol higher in energy than the lowest-energy *sp* crystal. Similarly, in the $Z' = 2$ search results, *sp* crystals are more common (99%) than *ap* crystals (1%). The preference for the *sp* conformer in predicted crystal structures is in agreement with experimental results. In all six known polymorphs of NIF, the molecular conformation is *sp* with respect to phenyl torsion. The same preference is observed in the solution of NIF at 303 K in which 90% of the molecules are *sp* and 10% are *ap*.²²

CONCLUSIONS

The newest polymorph of NIF (δ) had evaded detection for five decades and was discovered by the unorthodox method of pseudoseeding.⁶ Despite its unusual discovery in the lab, δ NIF was unveiled by standard CSP with a systematic search of the conformational space. This confirms the value of CSP as an important complement for experimental search for polymorphs. The predicted global minimum matches the most stable α NIF, while the other ordered structures are identified as low-energy structures (Ranks 3, 4, and 43). For NIF, it is important that the search be performed to cover both $Z' = 1$ and $Z' = 2$ structures; otherwise, the β and γ forms would have been missed.

As is the case with most CPS results,^{23,24} the predicted polymorphs of NIF outnumber the observed ones. In particular, of the four lowest-energy predicted structures, only Rank 2 has no experimental counterpart. This raises questions as to whether Rank 2 (and other low-energy structures) can be discovered experimentally or could be removed as a “redundant” structure that is equivalent or easily transformed to another. The CSP predicts many crystal structures built from the *trans/trans* conformer (Figure 3) and the *ap* conformer (Figure 4), while no such structures have been observed by experiment. To narrow the gap between

experiment and computation, there have been examples of new crystallization conditions leading to new polymorphs.^{10,25–30} On the computational side, kinetic factors can be taken into account to eliminate unviable structures, for example, short-lived structures due to fast polymorphic transition.

A significant limitation of the experimental mapping of the crystal energy landscape is survival; that is, we have data on the structures with high enough stability and fast enough crystallization rates to be observed, not those that are difficult to observe or not yet discovered. This leads to a sampling bias that frustrates the investigation of many long-standing questions in solid-state chemistry; for example, are racemic compounds generally denser and more stable than conglomerates?^{31–33} What is the energetic penalty to crystallize a polar structure relative to a nonpolar structure?³⁴ What is the energetic cost of building crystals with one conformer as opposed to another?³⁵ Experimental studies of these questions are necessarily limited by the structures that can be observed, but the answers may require the structures that are not (yet) observed. In this work, we used the results of our “computer experiments” to investigate the last of the questions above, showing how a given conformer of NIF is favored over others as a unit of crystal construction and the relative usage of different conformers in predicted structures. This understanding would be difficult to attain by experiment since the needed information on less stable structures is unavailable. In the same way, the CSP could be utilized to investigate the other questions above without limitations imposed by survival.

■ ASSOCIATED CONTENT

SI Supporting Information

The Supporting Information is available free of charge at <https://pubs.acs.org/doi/10.1021/acs.cgd.1c01317>.

CIFs from the CSP calculations as a compressed file (ZIP)

Lattice energy ranking table from the CSP calculations (XLSX)

■ AUTHOR INFORMATION

Corresponding Authors

Yue Gui — *School of Pharmacy, University of Wisconsin-Madison, Madison, Wisconsin 53705, United States*;  orcid.org/0000-0002-4416-3907; Email: ygui.wisc@gmail.com

Lian Yu — *School of Pharmacy, University of Wisconsin-Madison, Madison, Wisconsin 53705, United States*;  orcid.org/0000-0002-4253-5658; Email: lian.yu@wisc.edu

Authors

Yingdi Jin — *XtalPi Inc. (Shenzhen Jingtai Technology Co., Ltd.), Shenzhen 518100, China*

Shigang Ruan — *XtalPi Inc. (Shenzhen Jingtai Technology Co., Ltd.), Shenzhen 518100, China*

Guangxu Sun — *XtalPi Inc. (Shenzhen Jingtai Technology Co., Ltd.), Shenzhen 518100, China*

Vilmali López-Mejías — *Crystallization Design Institute, Molecular Sciences Research Center, University of Puerto Rico, San Juan, Puerto Rico 00926, United States; Department of Chemistry, University of Puerto Rico — Río Piedras Campus, San Juan, Puerto Rico 00931, United States*;  orcid.org/0000-0003-2138-8414

Complete contact information is available at: <https://pubs.acs.org/10.1021/acs.cgd.1c01317>

Notes

Y.G. is currently an employee of AbbVie. AbbVie did not participate in the development of this manuscript, and all work was done prior to Y.G.’s employment at AbbVie. The authors declare no competing financial interest.

■ ACKNOWLEDGMENTS

We thank the NSF-funded Wisconsin–Puerto Rico Partnership for Research and Education in Materials (NSF DMR-1827894) for supporting this work.

■ DEDICATION

We dedicate this work to Roger Davey.

■ REFERENCES

- (1) *World Health Organization Model List of Essential Medicines, 21st List*; World Health Organization, 2019.
- (2) Edraki, N.; Mehdipour, A. R.; Khoshneviszadeh, M.; Miri, R. Dihydropyridines: evaluation of their current and future pharmacological applications. *Drug Discovery Today* **2009**, *14*, 1058–1066.
- (3) Eckert, T.; Müller, J. Über polymorphe Modifikationen des Nifedipine aus underkühlten Schmelzen. [On polymorphic modifications of nifedipine from supercooled melts.]. *Arch. Pharm.* **1977**, *310*, 116–118.
- (4) Triggle, A. M.; Shefter, E.; Triggle, D. J. Crystal structures of calcium channel antagonists: 2,6-dimethyl-3,5-dicarbomethoxy-4-[2-nitro-, 3-cyano-, 4-(dimethylamino)-, and 2,3,4,5,6-pentafluorophenyl]-1,4-dihydropyridine. *J. Med. Chem.* **1980**, *23*, 1442–1445.
- (5) Gunn, E.; Guzei, I. A.; Cai, T.; Yu, L. polymorphism of nifedipine: crystal structure and reversible transition of the metastable β polymorph. *Cryst. Growth Des.* **2012**, *12*, 2037–2043.
- (6) Gui, Y.; Yao, X.; Guzei, I. A.; Aristov, M. M.; Yu, J.; Yu, L. A mechanism for reversible solid-state transitions involving nitro torsion. *Chem. Mater.* **2020**, *32*, 7754–7765.
- (7) Dunitz, J. D.; Bernstein, J. Disappearing polymorphs. *Acc. Chem. Res.* **1995**, *28*, 193–200.
- (8) Bučar, D.-K.; Lancaster, R. W.; Bernstein, J. Disappearing polymorphs revisited. *Angew. Chem., Int. Ed. Engl.* **2015**, *54*, 6972–6993.
- (9) Bauer, J.; Spanton, S.; Henry, R.; Quick, J.; Dziki, W.; Porter, W.; Morris, J. Ritonavir: an extraordinary example of conformational polymorphism. *Pharm. Res.* **2001**, *18*, 859–866.
- (10) Chen, S.; Guzei, I. A.; Yu, L. New polymorphs of ROY and new record for coexisting polymorphs of solved structures. *J. Am. Chem. Soc.* **2005**, *127*, 9881–9885.
- (11) Price, S. L.; Brandenburg, J. G. Molecular crystal structure prediction. In *Non-Covalent Interactions in Quantum Chemistry and Physics: Theory and Application*; de la Roza, A. O., DiLabio, G. A., Eds.; Elsevier: Amsterdam, 2017; pp 333–363.
- (12) Neumann, M. A.; Leusen, F. J. J.; Kendrick, J. A major advance in crystal structure prediction. *Angew. Chem., Int. Ed.* **2008**, *47*, 2427–2430.
- (13) Nyman, J.; Yu, L.; Reutzel-Edens, S. M. Accuracy and reproducibility in crystal structure prediction: the curious case of ROY. *CrystEngComm.* **2019**, *21*, 2080–2088.
- (14) Zhang, P.; Wood, G. P. F.; Ma, J.; Yang, M.; Liu, Y.; Sun, G.; Jiang, Y. A.; Hancock, B. C.; Wen, S. Harnessing cloud architecture for crystal structure prediction calculations. *Cryst. Growth Des.* **2018**, *18*, 6891–6900.
- (15) Kresse, G.; Hafner, J. Ab initio molecular dynamics for liquid metals. *Phys. Rev. B* **1993**, *47*, 558–561.
- (16) Kresse, G.; Furthmüller, J. Efficiency of *ab-initio* total energy calculations for metals and semiconductors using a plane-wave basis set. *Comput. Mater. Sci.* **1996**, *6*, 15–50.

(17) Kresse, G.; Hafner, J. Ab initio molecular-dynamics simulation of the liquid-metal–amorphous-semiconductor transition in germanium. *Phys. Rev. B* **1994**, *49*, 14251–14269.

(18) Perdew, J. P.; Burke, K.; Ernzerhof, M. Generalized gradient approximation made simple. *Phys. Rev. Lett.* **1996**, *77*, 3865–3868.

(19) Klimeš, J.; Bowler, D. R.; Michaelides, A. Van der Waals density functionals applied to solids. *Phys. Rev. B* **2011**, *83*, 195131.

(20) Gui, Y. Phase transitions in molecular solids: Understanding polymorphic transformation and crystal nucleation, and engineering amorphous drugs for global health. ProQuest Dissertations Publishing, Ph.D. thesis, University of Wisconsin-Madison, 2021.

(21) Goldmann, S.; Stoltefuss, J. 1,4-Dihydropyridines: Effects of chirality and conformation on the calcium antagonist and calcium agonist activities. *Angew. Chem., Int. Ed. Engl.* **1991**, *30*, 1559–1578.

(22) Rovnyak, G.; Andersen, N.; Gougoutas, J.; Hedberg, A.; Kimball, S. D.; Malley, M.; Moreland, S.; Porubcan, M.; Pudzianowski, A. Studies directed toward ascertaining the active conformation of 1,4-dihydropyridine calcium entry blockers. *J. Med. Chem.* **1988**, *31*, 936–944.

(23) Vasileiadis, M.; Kazantsev, A. V.; Karamertzanis, P. G.; Adjiman, C. S.; Pantelides, C. C. The polymorphs of ROY: application of a systematic crystal structure prediction technique. *Acta Crystallogr.* **2012**, *B68*, 677–685.

(24) Yao, C.; Guzei, I. A.; Jin, Y.; Ruan, S.; Sun, G.; Gui, Y.; Wang, L.; Yu, L. Polymorphism of piroxicam: new polymorphs by melt crystallization and crystal structure prediction. *Cryst. Growth Des.* **2020**, *20*, 7874–7881.

(25) López-Mejías, V.; Kampf, J. W.; Matzger, A. J. Nonamorphism in flufenamic acid and a new record for a polymorphic compound with solved structures. *J. Am. Chem. Soc.* **2012**, *134*, 9872–9875.

(26) Tyler, A. R.; Raghbir Singh, R.; McMonagle, C. J.; Waddell, P. G.; Heaps, S. E.; Steed, J. W.; Thaw, P.; Hall, M. J.; Probert, M. R. Encapsulated nanodroplet crystallization of organic-soluble small molecules. *Chem.* **2020**, *6*, 1755–1765.

(27) Lévesque, A.; Maris, T.; Wuest, J. D. ROY reclaims its crown: new ways to increase polymorphic diversity. *J. Am. Chem. Soc.* **2020**, *142*, 11873–11883.

(28) Roy, S.; Goud, N. R.; Matzger, A. J. Polymorphism in phenobarbital: discovery of a new polymorph and crystal structure of elusive form V. *Chem. Commun.* **2016**, *52*, 4389–4392.

(29) Case, D. H.; Srirambhatla, V. K.; Guo, R.; Watson, R. E.; Price, L. S.; Polyzois, H.; Cockcroft, J. K.; Florence, A. J.; Tocher, D. A.; Price, S. L. Successful computationally directed templating of metastable pharmaceutical polymorphs. *Cryst. Growth Des.* **2018**, *18*, 5322–5331.

(30) Bhardwaj, R. M.; McMahon, J. A.; Nyman, J.; Price, L. S.; Konar, S.; Oswald, I. D. H.; Pulham, C. R.; Price, S. L.; Reutzel-Edens, S. M. A prolific solvate former, galunisertib, under the pressure of crystal structure prediction, produces ten diverse polymorphs. *J. Am. Chem. Soc.* **2019**, *141*, 13887–13897.

(31) Jacques, J.; Collet, A.; Wilen, S. H. *Enantiomers, Racemates, and Resolutions*; Krieger Publishing Company: Malabar, FL, 1991.

(32) Brock, C. P.; Schweizer, W. B.; Dunitz, J. D. On the validity of Wallach's rule: on the density and stability of racemic crystals compared with their chiral counterparts. *J. Am. Chem. Soc.* **1991**, *113*, 9811–9820.

(33) Huang, J.; Yu, L. Effect of molecular chirality on racemate stability: α -amino acids with nonpolar R groups. *J. Am. Chem. Soc.* **2006**, *128*, 1873–1878.

(34) Hulliger, J.; Roth, S. W.; Quintel, A.; Bebie, H. Polarity of organic supramolecular materials: a tunable crystal property. *J. Solid State Chem.* **2000**, *152*, 49–56.

(35) Yu, L.; Stephenson, G. A.; Mitchell, C. A.; Bunnell, C. A.; Snorek, S. V.; Bowyer, J. J.; Borchardt, T. B.; Stowell, J. G.; Byrn, S. R. Thermochemistry and conformational polymorphism of a hexamorphic crystal system. *J. Am. Chem. Soc.* **2000**, *122*, 585–591.

□ Recommended by ACS

Elucidating the Structure of Ranitidine Hydrochloride Form II: Insights from Solid-State Spectroscopy and Ab Initio Simulations

Kacper Drużbicki, Jan Waśicki, *et al.*

JULY 03, 2018

CRYSTAL GROWTH & DESIGN

READ ▶

Order–Disorder Phase Transition between High- and Low-Z' Crystal Structures of the P1 Space Group

Ryusei Oketani, Hirohito Tsue, *et al.*

JANUARY 18, 2022

CRYSTAL GROWTH & DESIGN

READ ▶

Conformations in Solution and in Solid-State Polymorphs: Correlating Experimental and Calculated Nuclear Magnetic Resonance Chemical Shifts for Tol...

Helen Blade, Anjali K. Menakath, *et al.*

SEPTEMBER 18, 2020

THE JOURNAL OF PHYSICAL CHEMISTRY A

READ ▶

Elucidating the Dehydration Mechanism of Nitrofurantoin Monohydrate II Using Low-Frequency Raman Spectroscopy

Peter III J. G. Remoto, Keith C. Gordon, *et al.*

MARCH 15, 2022

CRYSTAL GROWTH & DESIGN

READ ▶

Get More Suggestions >